0022-3565/11/3391-286–297$25.00
THE JOURNAL OF PHARMACOLOGY AND EXPERIMENTAL THERAPEUTICS
JPET 339:286–297, 2011

Vol. 339, No. 1
184770/3719370
Printed in U.S.A.

Novel *N*-1,2-Dihydroxypropyl Analogs of Lobelane Inhibit Vesicular Monoamine Transporter-2 Function and Methamphetamine-Evoked Dopamine Release

David B. Horton, Kiran B. Siripurapu, Guangrong Zheng, Peter A. Crooks, and Linda P. Dwoskin

Department of Pharmaceutical Sciences, College of Pharmacy, University of Kentucky, Lexington, Kentucky

Received June 3, 2011; accepted July 20, 2011

ABSTRACT

Lobelane, a chemically defunctionalized saturated analog of lobeline, has increased selectivity for the vesicular monoamine transporter 2 (VMAT2) compared with the parent compound. Lobelane inhibits methamphetamine-evoked dopamine (DA) release and decreases methamphetamine self-administration. Unfortunately, tolerance develops to the ability of lobelane to decrease these behavioral effects of methamphetamine. Lobelane has low water solubility, which is problematic for drug development. The aim of the current study was to determine the pharmacological effect of replacement of the *N*-methyl moiety with a chiral *N*-1,2-dihydroxypropyl (*N*-1,2-diol) moiety, which enhances water solubility, altering the configuration of the *N*-1,2-diol moiety and incorporating phenyl ring substituents into the analogs. To determine VMAT2 selectivity, structure-activity relationships also were generated for inhibition of DA and serotonin transporters. Analogs with the highest potency for inhibiting DA uptake at VMAT2 and at least 10-fold selectivity were evaluated further for ability to inhibit methamphetamine-evoked DA release from superfused striatal slices. (*R*)-3-[2,6-*cis*-di(4-methoxyphenethyl)piperidin-1-yl]propane-1,2-diol (GZ-793A), the (*R*)-4-methoxyphenyl-*N*-1,2-diol analog, and (*R*)-3-[2,6-*cis*-di(1-naphthylethyl)piperidin-1-yl]propane-1,2-diol (GZ-794A), the (*R*)-1-naphthyl-*N*-1,2-diol analog, exhibited the highest potency (K_i ~30 nM) inhibiting VMAT2, and both analogs inhibited methamphetamine-evoked endogenous DA release (IC_{50} = 10.6 and 0.4 μM, respectively). Thus, the pharmacophore for VMAT2 inhibition accommodates the *N*-1,2-diol moiety, which improves drug-likeness and enhances the potential for the development of these clinical candidates as treatments for methamphetamine abuse.

Introduction

Methamphetamine is a highly addictive stimulant with robust rewarding properties leading to its abuse. Methamphetamine use continues to be a major health concern in the United States, with 100,000 new users in the United States every year (Substance Abuse and Mental Health Services Administration, Office of Applied Studies, 2008). To date, there are no approved therapeutics for methamphetamine

This work was supported by the National Institutes of Health National Institute on Drug Abuse [Grants DA13519, DA016176].

The University of Kentucky holds patents on lobeline and the analogs described in the current work, which have been licensed by Yaupon Therapeutics, Inc. A potential royalty stream to D.B.H., G.Z., P.A.C., and L.P.D. may occur consistent with University of Kentucky policy. Both P.A.C. and L.P.D. are founders of, and have financial interest in, Yaupon Therapeutics, Inc.

Article, publication date, and citation information can be found at http://jpet.aspetjournals.org.

doi:10.1124/jpet.111.184770.

ABBREVIATIONS: DAT, dopamine transporter; 5-HT, 5-hydroxytryptamine (serotonin); ANOVA, analysis of variance; DA, dopamine; DTBZ, dihydrotetrabenazine; EC, electrochemical detection; GBR 12909, 1-(2-(bis-(4-fluorophenyl)methoxy)ethyl)-4-(3-phenylpropyl)piperazine; GZ-252C, para-methoxyphenyl lobelane; GZ-745A, (*R*)-3-(2,6-*cis*-diphenethylpiperidin-1-yl)propane-1,2-diol; GZ-745B, (*S*)-3-(2,6-*cis*-diphenethylpiperidin-1-yl)propane-1,2-diol; GZ-790A, (*R*)-3-[2,6-*cis*-di(3-methoxyphenethyl)piperidin-1-yl]propane-1,2-diol; GZ-790B, (*S*)-3-[2,6-*cis*-di(3-methoxyphenethyl)piperidin-1-yl]propane-1,2-diol; GZ-791A, (*R*)-3-[2,6-*cis*-di(3-fluorophenethyl)piperidin-1-yl]propane-1,2-diol; GZ-791B, (*S*)-3-[2,6-*cis*-di(3-fluorophenethyl)piperidin-1-yl]propane-1,2-diol; GZ-792A, (*R*)-3-[2,6-*cis*-di(2-methoxyphenethyl)piperidin-1-yl]propane-1,2-diol; GZ-792B, (*S*)-3-[2,6-*cis*-di(2-methoxyphenethyl)piperidin-1-yl]propane-1,2-diol; GZ-793A, (*R*)-3-[2,6-*cis*-di(4-methoxyphenethyl)piperidin-1-yl]propane-1,2-diol; GZ-793B, (*S*)-3-[2,6-*cis*-di(4-methoxyphenethyl)piperidin-1-yl]propane-1,2-diol; GZ-794A, (*R*)-3-[2,6-*cis*-di(1-naphthylethyl)piperidin-1-yl]propane-1,2-diol; GZ-794B, (*S*)-3-[2,6-*cis*-di(1-naphthylethyl)piperidin-1-yl]propane-1,2-diol; GZ-795A, (*R*)-3-[2,6-*cis*-di(2,4-dichlorophenethyl)piperidin-1-yl]propane-1,2-diol; GZ-795B, (*S*)-3-[2,6-*cis*-di(2,4-dichlorophenethyl)piperidin-1-yl]propane-1,2-diol; GZ-796A, (*R*)-3-[2,6-*cis*-di(4-biphenylethyl)piperidin-1-yl]propane-1,2-diol; GZ-796B, (*S*)-3-[2,6-*cis*-di(4-biphenylethyl)piperidin-1-yl]propane-1,2-diol; GZ-797A, (*R*)-3-[2,6-*cis*-di(3,4-methylenedioxyphenethyl)piperidin-1-yl]propane-1,2-diol; GZ-797B, (*S*)-3-[2,6-*cis*-di(3,4-methylenedioxyphenethyl)piperidin-1-yl]propane-1,2-diol; HPLC, high-performance liquid chromatography; *N*-1,2-diol, *N*-1,2-dihydroxypropyl; Ro-4-1284, (2*R*,3*S*,11*bS*)-2-ethyl-3-isobutyl-9,10-dimethoxy-2,2,4,6,7,11*b*-hexahydro-1*H*-pyrido[2,1-*a*]isoquinolin-2-ol; SAR, structure-activity relationship; SERT, serotonin transporter; UKCP-110, *cis*-2,5-di-(2-phenethyl)-pyrrolidine hydrochloride; UKMH-106, (3Z,5Z)-3,5-bis(2,4-dichlorobenzylidene)-1-methylpiperidine; VMAT2, vesicular monoamine transporter 2.

abuse. Methamphetamine acts at both the dopamine transporter (DAT) and the vesicular monoamine transporter 2 (VMAT2) to increase extracellular dopamine (DA) concentrations (Sulzer et al., 2005). Specifically, methamphetamine reverses DA translocation by DAT to increase extracellular DA concentrations leading to reward (Fischer and Cho, 1979; Liang and Rutledge, 1982; Wise and Bozarth, 1987; Di Chiara and Imperato, 1988). Numerous studies have focused on DAT as a therapeutic target for the development of treatments for psychostimulant abuse (Grabowski et al., 1997; Dar et al., 2005; Howell et al., 2007; Tanda et al., 2009). However, this approach to drug discovery has thus far not resulted in viable efficacious therapeutics for methamphetamine abuse.

Methamphetamine inhibits DA uptake at VMAT2 and stimulates DA release from presynaptic vesicles, which presumably increases cytosolic DA concentrations (Sulzer and Rayport, 1990; Pifl et al., 1995; Sulzer et al., 1995). Taking into account VMAT2 as a component of the mechanism of action of methamphetamine, our research focus has been the discovery of novel therapeutic agents that target VMAT2. Structure-activity relationships (SARs) have been generated to elucidate novel pharmacophores that modify VMAT2 function with the aim of developing effective treatments for methamphetamine abuse (Zheng et al., 2005a,b; Crooks et al., 2010; Nickell et al., 2010, 2011; Horton et al., 2011).

Lobeline (Fig. 1), the principal alkaloid in *Lobelia inflata*, inhibits the neurochemical and behavioral effects of methamphetamine through its interaction with VMAT2 (Teng et al., 1997, 1998; Harrod et al., 2001; Miller et al., 2001; Dwoskin and Crooks, 2002; Nickell et al., 2010). Lobeline inhibits [^{3}H]dihydrotetrabenazine (DTBZ) binding to VMAT2 (K_i = 0.90 μM), [^{3}H]DA uptake at VMAT2 (K_i = 0.88 μM; Teng et al., 1997, 1998), and methamphetamine-evoked DA release (IC_{50} = 0.42 μM), supporting the tenet that VMAT2 is a viable therapeutic target for the development of treatments for methamphetamine abuse. In further support of this hypothesis, lobeline decreases methamphetamine self-administration in rats (Harrod et al., 2001). It is noteworthy that lobeline is not self-administered (Harrod et al., 2003), suggesting that it will not have abuse liability. Recently, lobeline has completed phase Ib clinical trials demonstrating safety in methamphetamine abusers (www.clinicaltrials.gov, NCT00439504).

Initial SAR around the lobeline pharmacophore revealed that lobelane (Fig. 1), a chemically defunctionalized, saturated analog of lobeline, competitively inhibited DA uptake at VMAT2 and exhibited increased affinity and selectivity for

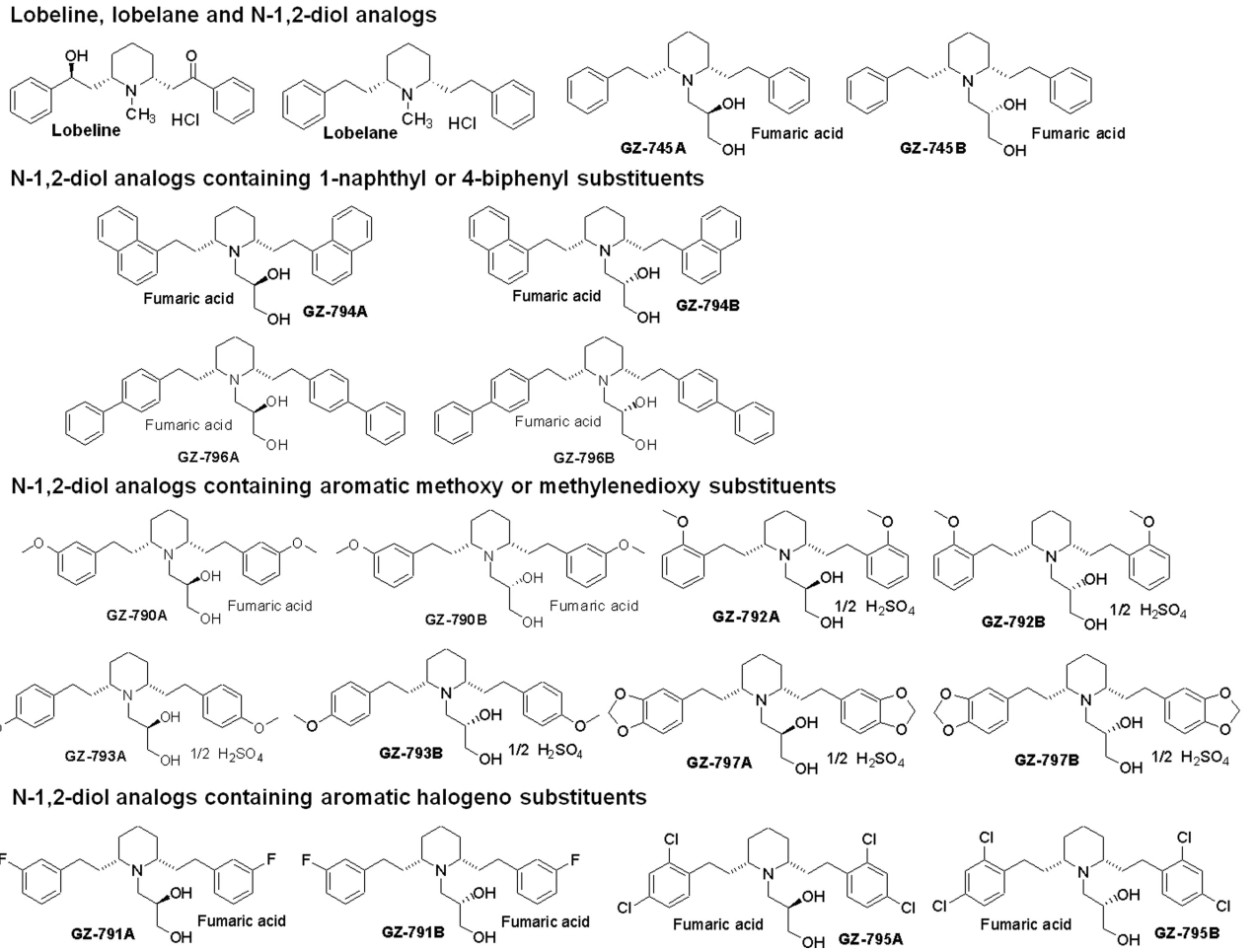

Fig. 1. Chemical structures of lobeline, lobelane, and *N*-1,2-diol analogs. For clarity of presentation, compounds are grouped according to structural similarity of substituent additions to the phenyl rings: lobeline, lobelane, and *N*-1,2-diol; *N*-1,2-diol analogs containing 1-naphthyl or 4-biphenyl substituents; *N*-1,2-diol analogs containing aromatic methoxy or methylenedioxy substituents; *N*-1,2-diol analogs containing aromatic halogeno substituents.

VMAT2 compared with lobeline (Miller et al., 2001; Nickell et al., 2010). Lobelane inhibited methamphetamine-evoked DA release and decreased methamphetamine self-administration; however, tolerance developed to the latter behavior effects (Neugebauer et al., 2007; Nickell et al., 2010). Unfortunately, lobelane exhibits decreased water solubility and diminished drug-likeness properties caused by its decreased polarity resulting from removal of the keto and hydroxyl functionalities of lobeline.

In the current study, the *N*-methyl moiety of the central piperidine ring of lobelane was replaced with a chiral *N*-1,2-dihydroxypropyl (*N*-1,2-diol) moiety to improve water solubility and enhance drug-likeness properties. Based on computational modeling, this structural modification was predicted to enhance water solubility. VMAT2 binding and function was determined after 1) replacement of the *N*-methyl moiety with a chiral *N*-1,2-diol moiety, 2) alteration of the configuration of the *N*-1,2-diol moiety, and 3) incorporation of phenyl ring substituents into the analogs. Specifically, incorporation of 2-methoxy, 3-methoxy, 4-methoxy, 3-flouro, 2,4-dichloro, and 3,4-methylenedioxy substituents into both phenyl rings, or replacement of the phenyl rings with naphthalene or biphenyl rings, were evaluated. To assess VMAT2 selectivity, SAR was generated for the inhibition of DAT and serotonin transporter (SERT) function. Analogs with the highest potency for inhibiting DA uptake at VMAT2 and with at least 10-fold selectivity were evaluated for the inhibition of methamphetamine-evoked DA release from superfused striatal slices. (*R*)-3-[2,6-*cis*-di(4-Methoxyphenethyl)piperidin-1-yl]propane-1,2-diol (GZ-793A) emerged as a potent, selective, and drug-like VMAT2 inhibitor to be further developed as a treatment for methamphetamine abuse.

Materials and Methods

Animals. Male Sprague-Dawley rats (200–250 g; Harlan, Indianapolis, IN) were housed two per cage with ad libitum access to food and water in the Division of Laboratory Animal Resources at the University of Kentucky (Lexington, KY). Experimental protocols involving the animals were in accord with the *Guide for the Care and Use of Laboratory Animals* (Institute of Laboratory Animal Resources, 1996) and approved by the Institutional Animal Care and Use Committee at the University of Kentucky.

Chemicals. [^{3}H]Dopamine ([^{3}H]DA; dihydroxyphenylethylamine, 3,4-[7-^{3}H]; specific activity, 28 Ci/mmol), [^{3}H]5-hydroxytryptamine ([^{3}H]5-HT; hydroxytryptamine creatinine sulfate 5-[1,2-^{3}H(N)]; specific activity, 30 Ci/mmol), and Microscint 20 LSC-cocktail were purchased from PerkinElmer Life and Analytical Sciences (Waltham, MA). [^{3}H]DTBZ [(±)α-[*O-methyl*-^{3}H]dihydrotetrabenazine; specific activity, 20 Ci/mmol] was obtained from American Radiolabeled Chemicals (St. Louis, MO). ATP-Mg^2, catechol, DA, EDTA, EGTA, fluoxetine HCl, 1-(2-(bis-(4-fluorophenyl)methoxy)ethyl)-4-(3-phenylpropyl)piperazine (GBR 12909), α-D-glucose, *S*-glycidol, *R*-glycidol, HEPES, $MgSO_4$, pargyline HCl, polyethyleneimine, KOH, potassium tartrate, and sucrose were purchased from Sigma-Aldrich (St. Louis, MO). L-Ascorbic acid and $NaHCO_3$ were purchased from Aldrich Chemical Co. (Milwaukee, WI). Ammonium hydroxide, $CaCl_2$, diethyl ether, KCl, K_2PO_4, methylene chloride, methanol, $MgCl_2$, NaCl, and NaH_2PO_4 were purchased from Thermo Fisher Scientific (Waltham, MA). Ethanol was purchased from Pharmco-AAPER Alcohol and Chemical Co., (Shelbyville, KY). Complete counting cocktail 3a70B was purchased from Research Products International (Mount Prospect, IL). (2*R*,3*S*,11*bS*)-2-Ethyl-3-isobutyl-9,10-dimethoxy-2,2,4,6,7,11*b*-hexahydro-1*H*-pyrido[2,1-*a*]isoquinolin-2-ol (Ro-4-1284) was a generous gift from Hoffman-LaRoche Inc. (Nutley, NJ).

General Synthetic Procedure for *N*-1,2-Diol Analogs. Based on computational modeling using ACD/ADME algorithms (www.acdlabs.com), replacement of the *N*-methyl moiety on the central piperidine ring with a *N*-1,2-diol moiety was predicted to enhance water solubility. For example, a 365% increase in water solubility was predicted as a consequence of replacing the *N*-methyl group in para-methoxyphenyl lobelane (GZ-252C) with an *N*-1,2-diol moiety in GZ-793A (solubility of 2.0 and 7.3 mg/ml in water, respectively; structures in Fig. 1 and Nickell et al., 2011). Synthesis of (*R*)-3-(2,6-*cis*-diphenethylpiperidin-1-yl)propane-1,2-diol (GZ-745A), which contains a *N*-1,2(*R*)-dihydroxylpropyl group, and (*S*)-3-(2,6-*cis*-diphenethylpiperidin-1-yl)propane-1,2-diol (GZ-745B), which contains a *N*-1,2(*S*)-dihydroxylpropyl group, was accomplished by reacting nor-lobelane with *S*-glycidol or *R*-glycidol in ethanol, respectively. The phenyl ring-modified nor-lobelane analogs were synthesized using previously reported methods (Zheng et al., 2005b), and the latter analogs served as intermediates for the synthesis of the current series of analogs via reaction with *S*-glycidol or *R*-glycidol in ethanol [i.e., (*R*)-3-[2,6-*cis*-di(3-methoxyphenethyl)piperidin-1-yl]propane-1,2-diol (GZ-790A), (*R*)-3-[2,6-*cis*-di(3-fluorophenethyl) piperidin-1-yl]propane-1,2-diol (GZ-791A), (*R*)-3-[2,6-*cis*-di(2-methoxyphenethyl)piperidin-1-yl]propane-1,2-diol (GZ-792A), GZ-793A, (*R*)-3-[2,6-*cis*-di(1-naphthylethyl)piperidin-1-yl]propane-1,2-diol (GZ-794A), (*R*)-3-[2,6-*cis*-di(2,4-dichlorophenethyl)piperidin-1-yl]propane-1,2-diol (GZ-795A), (*R*)-3-[2,6-*cis*-di(4-biphenylethyl)piperidin-1-yl]propane-1,2-diol (GZ-796A), and (*R*)-3-[2,6-*cis*-di(3,4-methylenedioxyphenethyl)piperidin-1-yl]propane-1,2-diol (GZ-797A), and the respective enantiomers (*S*)-3-[2,6-*cis*-di(3-methoxyphenethyl)piperidin-1-yl]propane-1,2-diol (GZ-790B), (*S*)-3-[2,6-*cis*-di(3-fluorophenethyl)piperidin-1-yl]propane-1,2-diol (GZ-791B), (*S*)-3-[2,6-*cis*-di(2-methoxyphenethyl)piperidin-1-yl]propane-1,2-diol (GZ-792B), (*S*)-3-[2,6-*cis*-di(4-methoxyphenethyl) piperidin-1-yl]propane-1,2-diol (GZ-793B), (*S*)-3-[2,6-*cis*-di(1-naphthylethyl)piperidin-1-yl]propane-1,2-diol (GZ-794B), (*S*)-3-[2,6-*cis*-di(2,4-dichlorophenethyl)piperidin-1-yl]propane-1,2-diol (GZ-795B), (*S*)-3-[2,6-*cis*-di(4-biphenylethyl)piperidin-1-yl]propane-1,2-diol (GZ-796B), and (*S*)-3-[2,6-*cis*-di(3,4-methylenedioxyphenethyl)piperidin-1-yl]propane-1,2-diol (GZ-797B)]. The final products were purified by silica gel column chromatography [eluting with methylene chloride/methanol/ammonium hydroxide, 30:1:0.2 (v/v/v)], followed by recrystallization from ethanol and diethyl ether after conversion into salt forms. Structures and purities of the analogs were determined by ^{1}H-NMR, ^{13}C-NMR, mass spectrometry, HPLC, and combustion analysis.

Synaptosomal [^{3}H]DA and [^{3}H]5-HT Uptake Assays. Analog-induced inhibition of [^{3}H]DA and [^{3}H]5-HT uptake into rat striatal and hippocampal synaptosomes, respectively, was determined using modifications of a previously described method (Horton et al., 2011). Brain regions were homogenized in 20 ml of ice-cold 0.32 M sucrose solution containing 5 mM $NaHCO_3$, pH 7.4, with 16 up-and-down strokes of a Teflon pestle homogenizer (clearance ~0.005 inch). Homogenates were centrifuged at 2000*g* for 10 min at 4°C, and resulting supernatants were centrifuged at 20,000*g* for 17 min at 4°C. Pellets were resuspended in 1.5 ml of Krebs' buffer, containing 125 mM NaCl, 5 mM KCl, 1.5 mM $MgSO_4$, 1.25 mM $CaCl_2$, 1.5 mM KH_2PO_4, 10 mM α-D-glucose, 25 mM HEPES, and 0.1 mM EDTA, with 0.1 mM pargyline and 0.1 mM ascorbic acid, saturated with 95% O_2/5% CO_2, pH 7.4. Synaptosomal suspensions (20 μg of protein/50 μl) were added to duplicate tubes containing 50 μl of analog (7–9 concentrations; 0.1 nM-1 mM, final concentration) and 350 μl of buffer and incubated at 34°C for 5 min in a total volume of 450 μl. Samples were placed on ice, and 50 μl of [^{3}H]DA or [^{3}H]5-HT (10 nM, final concentration) was added to each tube for a final volume of 500 μl. Reactions proceeded for 10 min at 34°C and were terminated by the addition of 3 ml of ice-cold Krebs' buffer. Nonspecific [^{3}H]DA and [^{3}H]5-HT uptake were determined in the presence of 10 μM GBR 12909 and 10 μM fluoxetine, respectively. Samples were rapidly filtered through Whatman (Clifton, NJ) GF/B filters using a cell harvester (MP-43RS; Brandel Inc., Gaithersburg, MD). Filters were washed three times with 4 ml of ice-cold Krebs' buffer containing catechol (1 mM). Complete counting cocktail was added to the filters,

and radioactivity was determined by liquid scintillation spectrometry (B1600 TR scintillation counter; PerkinElmer Life and Analytical Sciences).

[^{3}H]DTBZ Vesicular Binding Assays. Analog-induced inhibition of [^{3}H]DTBZ binding, a high-affinity ligand for VMAT2, was determined using modifications of a previously published method (Horton et al., 2011). Rat whole brain (excluding cerebellum) was homogenized in 20 ml of ice-cold 0.32 M sucrose solution with 10 up-and-down strokes of a Teflon pestle homogenizer (clearance ~0.008 inch). Homogenates were centrifuged at 1000*g* for 12 min at 4°C, and resulting supernatants were centrifuged at 22,000*g* for 10 min at 4°C. Resulting pellets were osmotically lyzed by incubation in 18 ml of cold water for 5 min. Osmolarity was restored by adding 2 ml of 25 mM HEPES and 100 mM potassium tartrate solution. Samples were centrifuged (20,000*g* for 20 min at 4°C), and then 1 mM $MgSO_4$ solution was added to the supernatants. Samples were centrifuged at 100,000*g* for 45 min at 4°C. Pellets were resuspended in cold assay buffer, containing 25 mM HEPES, 100 mM potassium tartrate, 5 mM $MgSO_4$, 0.1 mM EDTA, and 0.05 mM EGTA, pH 7.5. Assays were performed in duplicate using 96-well plates. Vesicular suspensions (15 μg of protein/100 μl) were added to wells containing 50 μl of analog (7–9 concentrations; 0.01 nM-0.1 mM, final concentration), 50 μl of buffer, and 50 μl of [^{3}H]DTBZ (3 nM, final concentration) for a final volume of 250 μl and incubated for 1 h at room temperature. Nonspecific binding was determined in the presence of 50 μl of 20 μM Ro-4-1284. Reactions were terminated by filtration onto Unifilter-96 GF/B filter plates (presoaked in 0.5% polyethyleneimine). Filters were washed three times with 350 μl of ice-cold buffer containing 25 mM HEPES, 100 mM potassium-tartrate, 5 mM $MgSO_4$, and 10 mM NaCl, pH 7.5. Filter plates were dried and bottom-sealed, and each well was filled with 40 μl of scintillation cocktail (MicroScint 20; PerkinElmer Life and Analytical Sciences). Radioactivity on the filters was determined by liquid scintillation spectrometry.

Vesicular [^{3}H]DA Uptake Assay. Analog-induced inhibition of [^{3}H]DA uptake into rat striatal vesicles was determined using modifications of a previously published method (Horton et al., 2011). Striata were homogenized in 14 ml of ice-cold 0.32 M sucrose solution containing 5 mM $NaHCO_3$, pH 7.4, with 10 up-and-down strokes of a Teflon pestle (clearance ~0.008 inch). Homogenates were centrifuged at 2000*g* for 10 min at 4°C, and resulting supernatants were centrifuged at 10,000*g* for 30 min at 4°C. Pellets were resuspended in 2.0 ml of 0.32 M sucrose and transferred to tubes containing 7 ml of MilliQ water and homogenized with five up-and-down strokes using the above homogenizer. Homogenates were transferred to tubes containing 900 μl of 0.25 M HEPES and 900 μl of 1.0 M potassium tartrate solution and centrifuged at 20,000*g* for 20 min at 4°C. Resulting supernatants were centrifuged at 55,000*g* for 60 min at 4°C. Subsequently, 100 μl of 1 mM $MgSO_4$, 100 μl of 0.25 M HEPES and 100 μl of 1.0 M potassium tartrate were added to the supernatant and centrifuged at 100,000*g* for 45 min at 4°C. Final pellets were resuspended in assay buffer, containing 25 mM HEPES, 100 mM potassium tartrate, 50 μM EGTA, 100 μM EDTA, 1.7 mM ascorbic acid, and 2 mM ATP-Mg-$^{2+}$, pH 7.4. Vesicular suspensions (10 μg of protein/100 μl) were added to duplicate tubes containing 50 μl of analog (7–9 concentrations; 1 nM-0.1 mM, final concentration), 300 μl of buffer, and 50 μl of [^{3}H]DA (0.1 μM, final concentration) for a final volume of 500 μl and incubated for 8 min at 34°C. Nonspecific [^{3}H]DA uptake was determined in the presence of 10 μM Ro-4-1284. Samples were filtered rapidly through Whatman GF/B filters using the cell harvester and washed three times with assay buffer containing 2 mM $MgSO_4$ in the absence of ATP. Radioactivity retained by the filters was determined as described under *Synaptosomal [^{3}H]DA and [^{3}H]5-HT Uptake Assays.*

Kinetics of Vesicular [^{3}H]DA Uptake. Vesicular suspensions were prepared as described above except that striata were pooled from two rats. Vesicular suspensions (20 μg of protein/50 μl) were added to duplicate tubes containing 25 μl of analog (final concentration approximating the K_i from inhibition curves for each analog), 150 μl of buffer, and 25 μl of various concentrations of [^{3}H]DA (1 nM–5 μM, final concentration) for a final volume of 250 μl and incubated for 8 min at 34°C. Nonspecific [^{3}H]DA uptake was determined using 10 μM Ro4-1284. Samples were processed as described under *Synaptosomal [^{3}H]DA and [^{3}H]5-HT Uptake Assays.*

Endogenous DA Release Assay. Rat coronal striatal slices of 0.5-mm thickness were prepared and incubated in Krebs' buffer, containing 118 mM NaCl, 4.7 mM KCl, 1.2 mM $MgCl_2$, 1.0 mM NaH_2PO_4, 1.3 mM $CaCl_2$, 11.1 mM α-D-glucose, 25 mM $NaHCO_3$, 0.11 mM L-ascorbic acid, and 0.004 mM EDTA, pH 7.4, saturated with 95% O_2/5% CO_2 at 34°C in a metabolic shaker for 60 min (Horton et al., 2011). Each slice was transferred to a glass superfusion chamber and superfused with Krebs' buffer at 1 ml/min for 60 min before sample collection. Two basal samples (1 ml) were collected at the 5- and 10-min time points. To determine the ability of analog to evoke DA overflow, each slice was superfused for 30 min in the absence or presence of a single concentration of analog (0.3–10 μM); analog was included in the buffer until the end of the experiment. Methamphetamine (5 μM) was added to the buffer after 30 min of superfusion, and slices were superfused for an additional 15 min with methamphetamine, followed by 20 min of superfusion in the absence of methamphetamine. In each experiment, a striatal slice was superfused for 90 min in the absence of both analog and methamphetamine, serving as the buffer control condition. In each experiment, duplicate slices were superfused with methamphetamine in the absence of analog, serving as the methamphetamine control condition. The methamphetamine concentration was selected based on pilot concentration-response data showing a reliable response of sufficient magnitude to allow evaluation of analog-induced inhibition. Each superfusate sample (1 ml) was collected into tubes containing 100 μl of 0.1 M perchloric acid. Before HPLC-EC analysis, ascorbate oxidase (20 μl, 168 U/mg reconstituted to 81 U/ml) was added to 500 μl of each sample and vortexed for 30 s, and 100 μl was injected onto the HPLC-EC system. The HPLC-EC system consisted of a pump (model 126; Beckman Coulter, Fullerton, CA) and autosampler (model 508; Beckman Coulter), an ODS Ultrasphere C18 reverse-phase 80 × 4.6 mm, 3-μm column, a Coulometric-II detector with guard cell (model 5020) maintained at + 0.60 V, and an analytical cell (model 5011) maintained at potentials E1 = −0.05 V and E2 = +0.32 V (ESA Inc., Chelmsford, MA). HPLC mobile phase (flow rate, 1.5 ml/min) was 0.07 M citrate/0.1 M acetate buffer, pH 4, containing 175 mg/l octylsulfonic acid sodium salt, 650 mg/l NaCl, and 7% methanol. Separations were performed at room temperature, and 5 to 6 min were required to process each sample. Retention times of DA standards were used to identify respective peaks. Peak heights were used to quantify the detected amounts of analyte based on standard curves. Detection limit for DA was 1 to 2 pg/100 μl.

Data Analysis. Specific [^{3}H]DTBZ binding and specific [^{3}H]DA and [^{3}H]5-HT uptake were determined by subtracting the nonspecific binding or uptake from the total binding or uptake, respectively. Analog concentrations that produced 50% inhibition of the specific binding or uptake (IC_{50} values) were determined from the concentration-effect curves via an iterative curve-fitting program (Prism 5.0; GraphPad Software Inc., San Diego, CA). Inhibition constants (K_i values) were determined using the Cheng-Prusoff equation (Cheng and Prusoff, 1973). For kinetic analyses, K_m and V_{max} were determined using one-site binding curves. Paired two-tailed *t* tests were performed on the arithmetic V_{max} and the log K_m values to determine significant differences between analog and control (absence of analog). Pearson's correlation analysis determined the relationship between affinity for the [^{3}H]DTBZ binding site and vesicular [^{3}H]DA uptake.

For endogenous neurotransmitter release assays, fractional release was defined as the DA concentration in each sample divided by the slice weight. Basal DA outflow was calculated as the average fractional release of the two basal samples collected 10 min before addition of analog to the buffer. Intrinsic DA overflow was calculated

as the sum of the increases in fractional release above basal outflow during superfusion with analog alone (in the absence of methamphetamine). One-way repeated-measures ANOVAs determined concentration-dependent effects on DA overflow. Peak DA fractional release evoked by methamphetamine was determined from the time course. Analog-induced inhibition of methamphetamine-evoked fractional DA release was evaluated using one-way repeated-measures ANOVA. When appropriate, Dunnett's post hoc test determined concentrations of analog that significantly decreased the effect of methamphetamine. Log IC_{50} value for each analog was generated using an iterative nonlinear least-squares curve-fitting program (Prism version 5.0). Statistical significance was defined as $p < 0.05$.

Results

***N*-1,2-Diol Analogs Inhibit [^{3}H]DA Uptake at DAT.** Concentration-response curves for GBR 12909, cocaine, lobeline, lobelane, and the *N*-1,2-diol analogs to inhibit [^{3}H]DA uptake into striatal synaptosomes are illustrated in Fig. 2. K_i values for GBR 12909, cocaine, lobeline, and lobelane (Table 1) are consistent with previously reported findings (Reith et al., 1994; Han and Gu, 2006; Nickell et al., 2010). Replacement of the *N*-methyl in lobelane with a *N*-1,2-diol moiety generally afforded analogs that were 1- to 10-fold less potent (K_i = 1.43–9.5 μM) at DAT compared with lobelane. Alteration of the configuration of the *N*-1,2-diol and incorporation of phenyl ring substitutents did not alter affinity for DAT. It is noteworthy that lead analogs, GZ-793A [4-methoxyphenyl-*N*-1,2(*R*)-diol analog] and GZ-794A [1-naphthalene-*N*-1,2(*R*)-diol analog], inhibited [^{3}H]DA uptake with potencies not different from lobelane.

***N*-1,2-Diol Analogs Inhibit [^{3}H]5-HT Uptake at SERT.** Concentration-response curves for fluoxetine, lobeline, lobelane, and the *N*-1,2-diol analogs to inhibit [^{3}H]5-HT uptake into hippocampal synaptosomes are illustrated in Fig. 3. K_i values for fluoxetine, lobeline, and lobelane (Table 1) are consistent with previously reported findings (Owens et al., 2001; Miller et al., 2004). Generally, replacement of the *N*-methyl moiety with the *N*-1,2-diol moiety, alteration of the configuration of the *N*-1,2-diol, and incorporation of phenyl ring substitutents did not alter affinity for SERT (K_i = 0.94–11.0 μM versus 3.6 μM). Exceptions include the 1-naphthalene enantiomers, GZ-794A and GZ-794B (K_i = 0.31 and 0.16 μM, respectively), which afforded a 10- to 20-fold increase in potency compared with lobelane. It is noteworthy that the lead compound, GZ-793A, exhibited potency not different from lobelane.

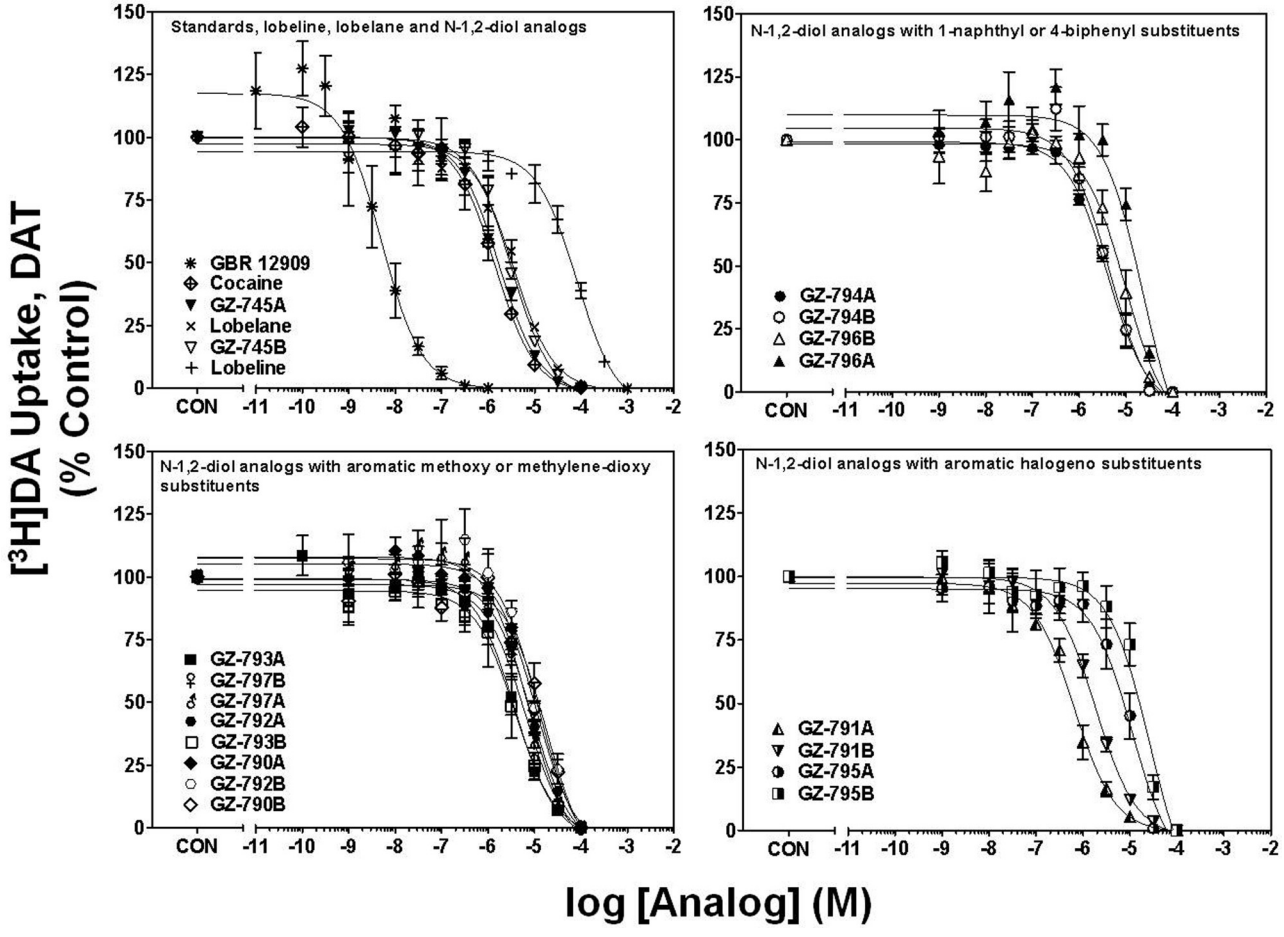

Fig. 2. *N*-1,2-Diol analogs inhibit [^{3}H]DA uptake into rat striatal synaptosomes. For clarity of presentation, compounds are grouped according to structural similarity of substituent additions to the phenyl rings: standards, lobeline, lobelane, and *N*-1,2-diol analogs (top left), *N*-1,2-diol analogs containing 1-naphthyl or 4-biphenyl substituents (top right), *N*-1,2-diol analogs containing aromatic methoxy or methylenedioxy substituents (bottom left), or *N*-1,2-diol analogs containing aromatic halogeno substituents (bottom right). Nonspecific [^{3}H]DA uptake was determined in the presence of 10 μM GBR 12909. Control (CON) represents specific [^{3}H]DA uptake in the absence of analog (19.3 ± 0.94 pmol/mg/min). Symbol inset shows compounds in order from highest to lowest affinity. n = 4 rats/analog.

TABLE 1
Summary for standards, lobeline, lobelane, and N-1,2-diol analogs

Compound	K_i ± S.E.M.			
	DAT, [^{3}H]DA Uptake	SERT, [^{3}H]5-HT Uptake	VMAT2, [^{3}H]DTBZ Binding	VMAT2, [^{3}H]DA Uptake
			μ*M*	
Standards				
GBR 12909	0.0009 ± 0.0001[a]	N.D.	N.D.	N.D.
Cocaine	0.48 ± 0.07	N.D.	N.D.	N.D.
Fluoxetine	N.D.	0.007 ± 0.0001[a]	N.D.	N.D.
Ro-4-1284	0.04 ± 0.005	0.02 ± 0.003	0.03 ± 0.003[a]	0.02 ± 0.002[a]
Lobeline, lobelane, and *N*-1,2-diol analogs				
Lobeline	28.2 ± 6.73	46.8 ± 3.70	2.04 ± 0.64[b]	1.27 ± 0.46
Lobelane	1.05 ± 0.03	3.60 ± 0.35	0.97 ± 0.19[b]	0.067 ± 0.007
GZ-745A	0.60 ± 0.06	8.43 ± 2.80	0.56 ± 0.08	0.19 ± 0.05
GZ-745B	1.08 ± 0.12	11.0 ± 3.12	1.28 ± 0.13	0.86 ± 0.12
N-1,2-Diol analogs containing 1-naphthyl or 4-biphenyl substituents				
GZ-794A	1.43 ± 0.14	0.31 ± 0.08	0.31 ± 0.07	0.033 ± 0.002
GZ-794B	1.57 ± 0.16	0.16 ± 0.04	0.13 ± 0.01	0.08 ± 0.01
GZ-796A	8.33 ± 1.46	5.30 ± 0.96	>100	0.79 ± 0.23
GZ-796B	3.43 ± 0.63	2.55 ± 0.77	90.2 ± 9.70	2.25 ± 1.30
N-1,2-Diol analogs containing aromatic methoxy or methylene-dioxy substituents				
GZ-790A	3.80 ± 0.69	3.14 ± 1.18	0.46 ± 0.22	0.14 ± 0.02
GZ-790B	6.67 ± 2.15	8.03 ± 2.30	2.73 ± 0.68	0.52 ± 0.04
GZ-792A	2.90 ± 0.23	1.33 ± 0.46	1.04 ± 0.73	0.49 ± 0.06
GZ-792B	4.77 ± 1.03	0.94 ± 0.14	1.87 ± 0.69	0.79 ± 0.08
GZ-793A	1.44 ± 0.27	9.36 ± 2.74	8.29 ± 2.79	0.029 ± 0.008
GZ-793B	3.40 ± 0.82	10.4 ± 2.75	7.74 ± 2.34	0.18 ± 0.04
GZ-797A	2.46 ± 0.16	2.10 ± 0.70	1.30 ± 0.05	0.16 ± 0.04
GZ-797B	2.21 ± 0.31	2.63 ± 0.60	5.61 ± 0.62	0.76 ± 0.04
N-1,2-Diol analogs containing aromatic halogeno substituents				
GZ-791A	0.25 ± 0.07	1.32 ± 0.46	1.00 ± 0.16	0.19 ± 0.06
GZ-791B	0.62 ± 0.05	2.87 ± 0.50	1.08 ± 0.38	1.03 ± 0.16
GZ-795A	3.87 ± 0.89	2.15 ± 0.38	10.4 ± 0.65	0.14 ± 0.04
GZ-795B	9.50 ± 2.53	1.86 ± 0.39	13.9 ± 0.38	0.09 ± 0.04

N.D., not determined.
[a] n = 3–4 rats.
[b] Data for [^{3}H]DTBZ binding for lobeline and lobelane taken from Nickell et al., 2010.

***N*-1,2-Diol Analogs Inhibit [^{3}H]DTBZ Binding at VMAT2.** Concentration-response curves for Ro-4-1284, lobeline, lobelane, and the *N*-1,2-diol analogs to inhibit [^{3}H]DTBZ binding to whole brain membranes are illustrated in Fig. 4, and K_i values are provided in Table 1. The K_i value for Ro-4-1284 to inhibit [^{3}H]DTBZ binding is consistent with previously reported results (Cesura et al., 1990). Generally, replacement of the *N*-methyl moiety with the *N*-1,2-diol moiety, alteration of the configuration of the *N*-1,2-diol, and incorporation of phenyl ring substitutents did not alter affinity for the [^{3}H]DTBZ site on VMAT2 (K_i = 0.46–5.6 μM versus 0.97 μM). It is noteworthy that GZ-794A [1-naphthalene *N*-1,2(*R*)-diol analog] exhibited potency not different from lobelane. Exceptions include the 4-methoxyphenyl enantiomers (GZ-793A and GZ-793B) and the 2,4-dichlorophenyl enantiomers (GZ-795A and GZ-795B), which exhibited 8- to 10-fold lower potency compared with lobelane. In addition, GZ-796A and GZ-796B, the 4-biphenyl enantiomers, exhibited 90- to 100-fold lower potency than lobelane.

***N*-1,2-Diol Analogs Inhibit [^{3}H]DA Uptake at VMAT2.** Concentration-response curves for Ro-4-1284, lobeline, lobelane, and the *N*-1,2-diol analogs to inhibit [^{3}H]DA uptake into striatal vesicles are illustrated in Fig. 5. K_i values for Ro-4-1284, lobeline, and lobelane (Table 1) are consistent with previous reports (Nickell et al., 2010). Replacement of the *N*-methyl moiety with the *N*-1,2-diol and incorporation of the phenyl ring substituents resulted in a 5- to 45-fold lower potency inhibiting [^{3}H]DA uptake at VMAT2 compared with lobelane. Exceptions include GZ-793A [4-methoxyphenyl *N*-1,2(*R*)-diol analog] and GZ-794A [1-naphthalene *N*-1,2(*R*)-diol analog], which were equipotent with lobelane. Generally, the *R*-configuration of the *N*-1,2-diol analogs was more potent than the *S*-configuration in inhibiting VMAT2 function. Correlation analysis revealed no correlation between the K_i values for inhibiting [^{3}H]DA uptake at VMAT2 and [^{3}H]DTBZ binding at VMAT2 (Pearson's correlation coefficient r = 0.37; p = 0.13; Fig. 6).

***N*-1,2-Diol Analogs Inhibit [^{3}H]DA Uptake at VMAT2 Competitively.** To elucidate the mechanism of inhibition at VMAT2, i.e., competitive or noncompetitive, kinetic analyses of [^{3}H]DA uptake at VMAT2 were conducted using the most potent analog inhibitors of VMAT2 function, i.e., GZ-793A and GZ-794A. GZ-793A had relatively low affinity for the [^{3}H]DTBZ binding site, whereas GZ-794A had high affinity for this site. For comparison, kinetic analysis of GZ-796A was performed to evaluate the mechanism of inhibition of an analog with moderate potency inhibiting DA uptake at VMAT2, but low potency at the [^{3}H]DTBZ binding site. Results show an increased K_m value with no change in V_{max} for each analog compared with control (Fig. 7), indicating a competitive mechanism of action.

***N*-1,2-Diol Analogs Inhibit Methamphetamine-Evoked Endogenous DA Release.** In the absence of methamphetamine, GZ-793A, GZ-794A, and GZ-796A did not evoke DA overflow above basal outflow (data not shown; one-way repeated measures ANOVA: $F_{5,29}$ = 0.31, 1.32, and 0.48, respectively; $p > 0.05$). It is noteworthy that GZ-793A, GZ-794A, and GZ-796A inhibited methamphetamine-evoked DA release in a concentration-dependent manner (Fig. 8; repeated measures one-way ANOVAs: $F_{5,29}$ = 4.55, 3.16, and 3.03, respectively;

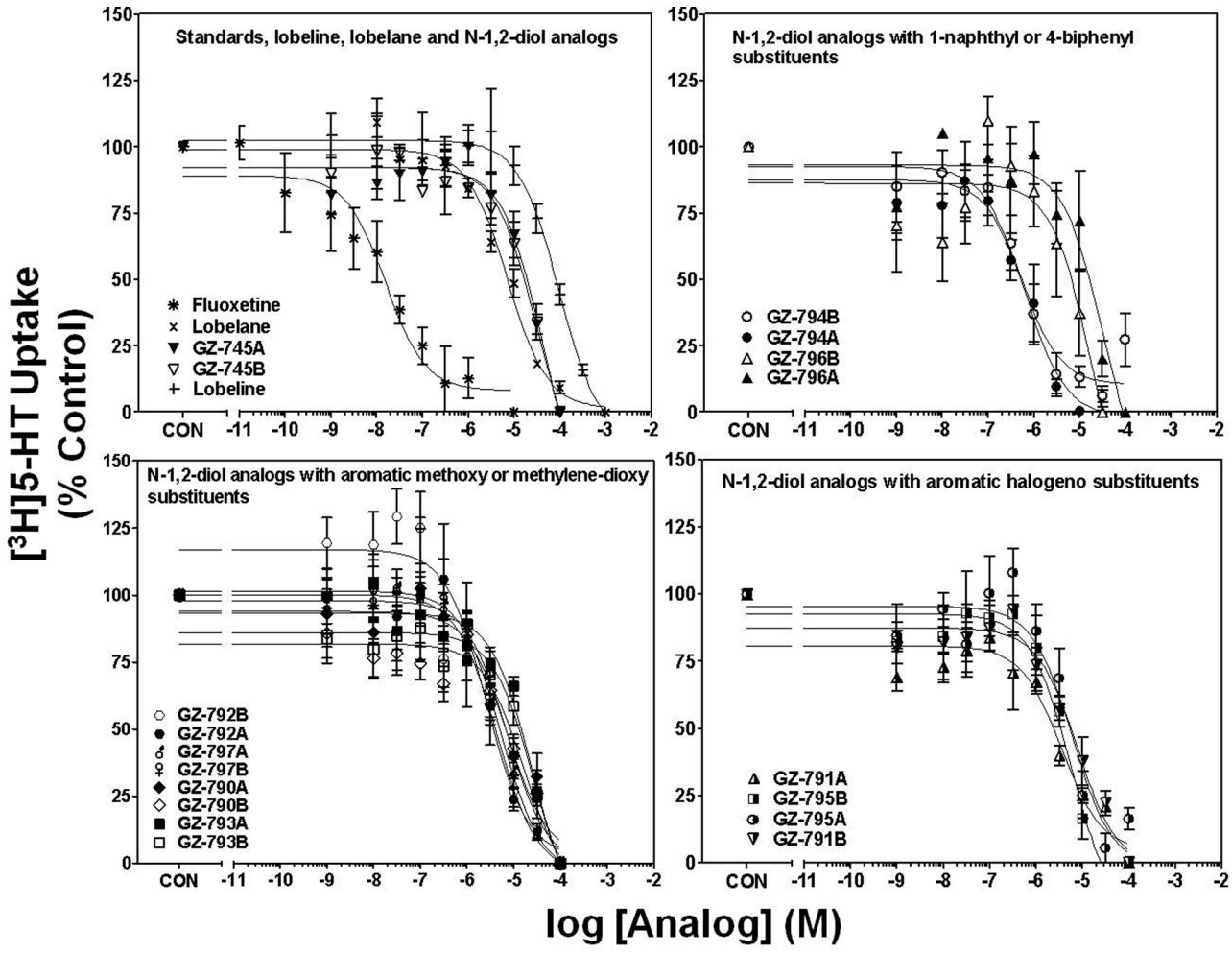

Fig. 3. *N*-1,2-Diol analogs inhibit [^{3}H]5-HT uptake into rat hippocampal synaptosomes. For clarity of presentation, compounds are grouped according to structural similarity of additions to the phenyl rings: standards, lobeline, lobelane, and *N*-1,2-diol analogs (top left), *N*-1,2-diol analogs containing 1-naphthyl or 4-biphenyl substituents (top right), *N*-1,2-diol analogs containing aromatic methoxy or methylenedioxy substituents (bottom left), or *N*-1,2-diol analogs containing aromatic halogeno substituents (bottom right). Nonspecific [^{3}H]5-HT uptake was determined in the presence of 10 μM fluoxetine. Control (CON) represents specific [^{3}H]5-HT uptake in the absence of analog (0.56 ± 0.06 pmol/mg/min). Symbol inset shows compounds in order from highest to lowest affinity. $n = 4$ rats/analog.

$p < 0.05$). Even though GZ-793A and GZ-794A inhibited DA uptake at VMAT2 equipotently, GZ-793A was 25-fold less potent than GZ-794A in inhibiting methamphetamine-evoked DA release. Furthermore, GZ-793A exhibited ~35% greater inhibitory activity compared with GZ-794A. Although GZ-796A had 25-fold lower potency than either GZ-793A or GZ-794A in inhibiting DA uptake at VMAT2, GZ-796A was equipotent with GZ-794A and 10-fold more potent than GZ-793A in inhibiting methamphetamine-evoked DA release. Inhibitory activity of GZ-796A (I_{max} = 56%) was not different from that exhibited by GZ-794A.

Discussion

The current study reports on the most recent phase of an iterative process of drug discovery aimed at identifying a novel lead candidate for the treatment of methamphetamine abuse. The rationale for VMAT2 as the pharmacological target evolved from the observation that methamphetamine interacts with this presynaptic protein to inhibit DA uptake into presynaptic vesicles. Inhibition of VMAT2 increases cytosolic DA levels available for methamphetamine-induced reverse transport by DAT, leading to an increase in extracellular DA (Sulzer et al., 2005). Through an interaction with VMAT2, lobeline inhibits the neurochemical and behavioral effects of methamphetamine (Teng et al., 1997, 1998; Harrod et al., 2001; Miller et al., 2001; Dwoskin and Crooks, 2002; Nickell et al., 2010). Lobelane, a lobeline analog with greater selectivity for VMAT2, decreased both methamphetamine-evoked DA release (IC_{50} = 0.65 μM; I_{max} = 73.2%; same experimental conditions as the current work) and methamphetamine self-administration (Zheng et al., 2005a; Neugebauer et al., 2007; Beckmann et al., 2010; Nickell et al., 2010, 2011). Unfortunately, further development of lobelane as an effective pharmacotherapy was hindered by unacceptable drug-likeness properties. The current study identified novel analogs of lobelane incorporating a *N*-1,2-diol moiety into the molecule to specifically enhance its drug-likeness properties. GZ-793A emerged as a potent, VMAT2-selective, drug-like lead candidate for the treatment of methamphetamine abuse.

The current SAR provided several insights regarding the optimization of the pharmacophore for inhibition of VMAT2 function (Tables 1 and 2). Merely replacing the *N*-methyl

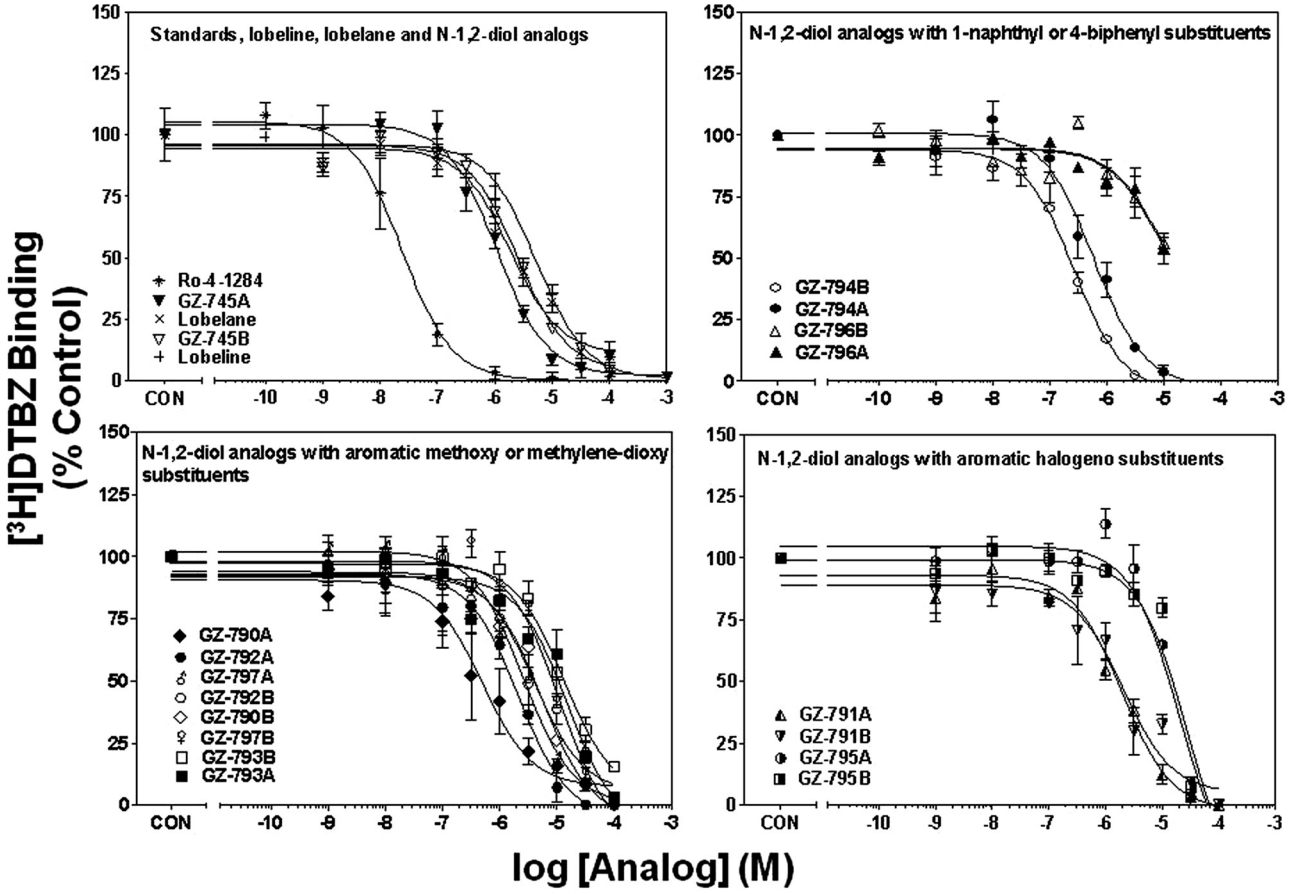

Fig. 4. *N*-1,2-Diol analogs inhibit [^{3}H]DTBZ binding to vesicle membranes from rat whole brain preparations. For clarity of presentation, compounds are grouped according to structural similarity of additions to the phenyl rings: standards, lobeline, lobelane, and *N*-1,2-diol analogs (top left), *N*-1,2-diol analogs containing 1-naphthyl or 4-biphenyl substituents (top right), *N*-1,2-diol analogs containing aromatic methoxy or methylenedioxy substituents (bottom left), or *N*-1,2-diol analogs containing aromatic halogeno substituents (bottom right). Nonspecific [^{3}H]DTBZ binding was determined in the presence of 10 μM Ro-4-1284. Control (CON) represents specific [^{3}H]DTBZ binding in the absence of analog (1.65 ± 0.05 pmol/mg protein). Symbol inset shows compounds in order from highest to lowest affinity. n = 4 rats/analog. Previous results for lobeline and lobelane were obtained from Nickell et al., 2010.

group of lobelane with a *N*-1,2(R)-diol moiety (GZ-745A) resulted in a 4-fold decrease in VMAT2 inhibitory potency. In addition, the specific configuration of the *N*-1,2-diol moiety is a factor determining potency to inhibit DA uptake at VMAT2. The *R* enantiomer of *N*-1,2-diol analogs bearing no phenyl substituents, and those containing 3-flourophenyl, 3-methoxyphenyl, 4-methoxyphenyl, or 3,4-methylenedioxyphenyl moieties exhibited 4- to 6-fold higher inhibitory potency compared with the corresponding *S* enantiomer. These results indicate that the pharmacophore for inhibition of VMAT2 function has a configurational restriction at the chiral *N*-1,2-diol moiety in the current series of analogs. Furthermore, *N*-1,2-diol analogs of lobelane with 3-fluoro, 2,4-dichloro, 2-methoxy, 3-methoxy, or 3,4-methylenedioxy substituents in both phenyl rings, or in which the phenyl rings were replaced with 1-naphthalene or 4-biphenyl rings, exhibited a 4- to 34-fold lower potency compared with lobelane and a 3- to 66-fold lower potency compared with the corresponding *N*-methyl substituted analog. Thus, although *N*-methyl analogs with substituents on the phenyl rings retained potency as inhibitors of VMAT2 relative to lobelane, introduction of these substituents into the phenyl rings in the *N*-1,2-diol analogs resulted in reduced potency. Exceptions included the two lead *N*-1,2(R)-diol analogs, GZ-793A (4-methoxyphenyl analog) and GZ-794A (1-naphthalene analog), which inhibited VMAT2 with potencies not different from either lobelane or the corresponding *N*-methyl analogs. These results indicate that for GZ-793A and GZ-794A structural modifications that enhanced drug-likeness did not alter VMAT2 inhibitory potency.

The use of [^{3}H]DTBZ to probe interaction with VMAT2 has been established in rodent models and in evaluation of patients with specific pathologies (Lehéricy et al., 1994; Kilbourn et al., 1995). However, studies have reported that inhibition of VMAT2 function does not correlate with affinity for the [^{3}H]DTBZ binding site on VMAT2 (Horton et al., 2011; Nickell et al., 2011). These latter studies evaluated the SAR for a series of phenyl ring substituted lobelane analogs and for conformationally restricted meso-transdiene analogs. Results obtained from the current series of novel *N*-1,2-diol analogs were consistent with the latter observations, i.e., a correlation was not observed between VMAT2 binding and uptake. Together, the SAR indicates that [^{3}H]DTBZ binding site is more tolerant of structural alterations relative to the uptake site on VMAT2. One analog in the current series [GZ-796A, the 4-biphenyl *N*-1,2(*R*)-diol analog], inhibited DA uptake at VMAT2, but did not inhibit [^{3}H]DTBZ binding, consistent with previous results that 4-biphenyl nor-lobelane

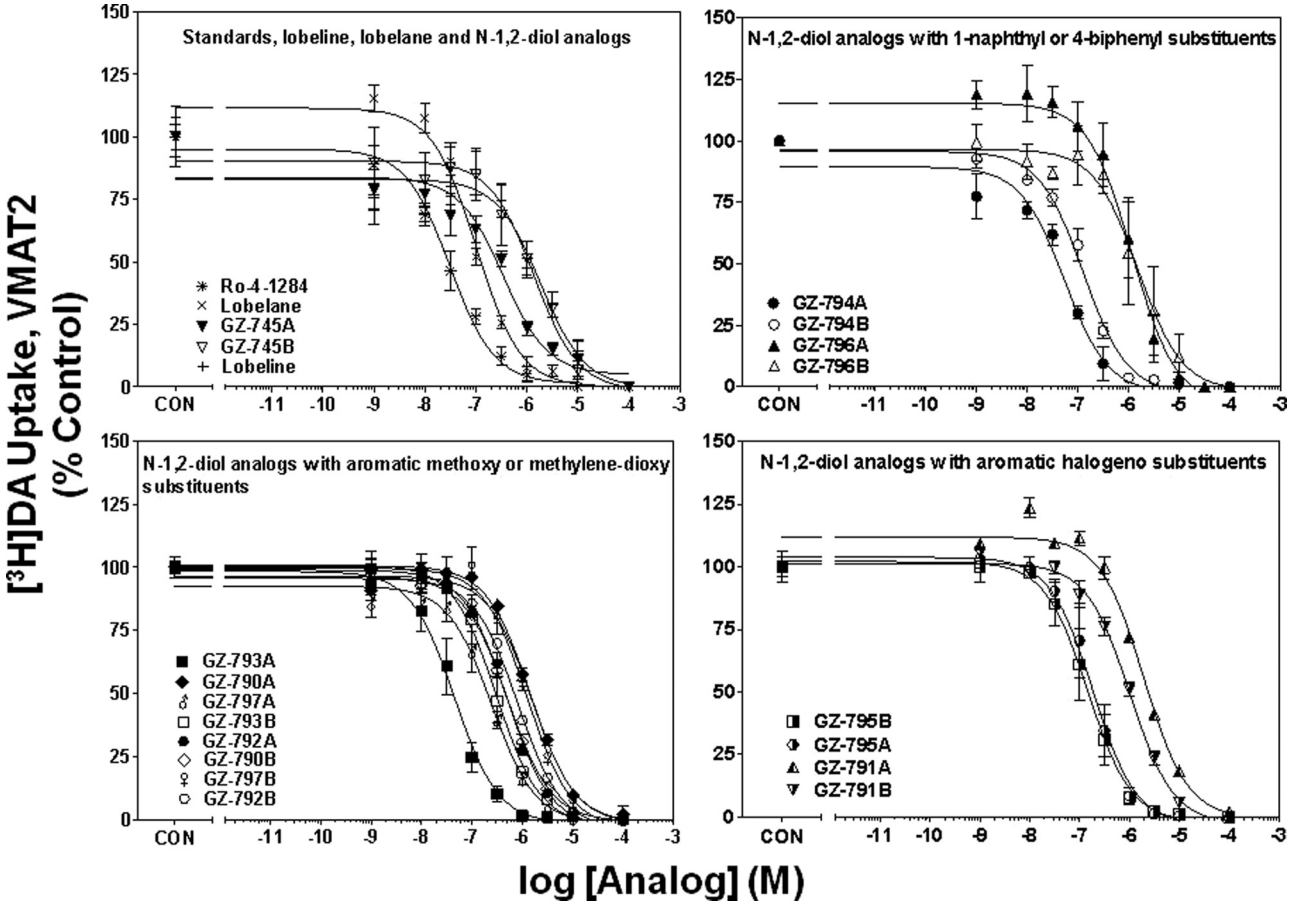

Fig. 5. *N*-1,2-Diol analogs inhibit [^{3}H]DA uptake into vesicles prepared from rat striatum. For clarity of presentation, compounds are grouped according to structural similarity of additions to the phenyl rings: standards, lobeline, lobelane, and *N*-1,2-diol analogs (top left), *N*-1,2-diol analogs containing 1-naphthyl or 4-biphenyl substituents (top right), *N*-1,2-diol analogs containing aromatic methoxy or methylenedioxy substituents (bottom left), or *N*-1,2-diol analogs containing aromatic halogeno substituents (bottom right). Nonspecific [^{3}H]DA uptake was determined in the presence of 10 μM Ro-4-1284. Control (CON) represents specific vesicular [^{3}H]DA uptake in the absence of analog (34.1 ± 1.18 pmol/mg/min). Symbol inset shows compounds in order from highest to lowest affinity. $n = 4$ rats/analog.

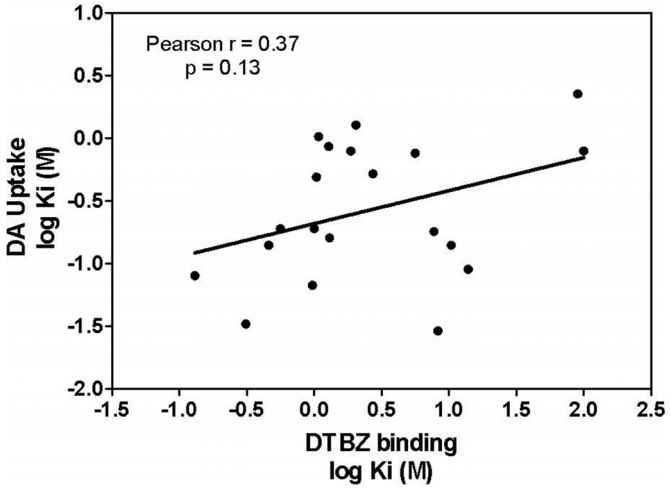

Fig. 6. Lack of correlation between *N*-1,2-diol analogs inhibition of [^{3}H]DTBZ binding and [^{3}H]DA uptake at VMAT2. Data presented are K_i values obtained from concentration-response curves for analog-induced inhibition of [^{3}H]DTBZ binding and [^{3}H]DA uptake at VMAT2 (Figs. 4 and 5, respectively). Pearson's correlation analysis revealed a lack of correlation (Pearson's correlation coefficient $r = 0.37$; $p = 0.13$) between the ability of *N*-1,2-diol analogs to inhibit [^{3}H]DTBZ binding to VMAT2 and [^{3}H]DA uptake at VMAT2.

as well as several extensively aromatized *N*-methyl lobelane analogs inhibited VMAT2 function, but not [^{3}H]DTBZ binding (Nickell et al., 2011). Thus, analogs in these structural series seem to interact with two distinct sites on VMAT2.

Although VMAT2 and plasma membrane transporters (e.g., DAT and SERT) belong to two different transporter families and exhibit little structural homology (Liu and Edwards, 1997), these proteins are promiscuous and translocate DA and 5-HT (Norrholm et al., 2007), suggesting that there are similarities in the substrate sites between these transporters. Because the parent compound lobelane exhibited only 15-fold selectivity for VMAT2 over DAT and SERT, it was imperative to assess interaction of the *N*-1,2-diol analogs with DAT and SERT to ascertain selectivity for VMAT2. Only the 1-naphthalene analogs exhibited a 10-fold higher potency inhibiting SERT compared with lobelane, whereas the remainder of the series of *N*-1,2-diol analogs exhibited affinity not different from lobelane at both DAT and SERT. Configuration of the *N*-1,2-diol moiety influenced potency to inhibit VMAT2 function, but did not influence potency at DAT and SERT.

The next critical step in our drug discovery approach was to determine the ability of the lead compounds to inhibit the neurochemical effects of methamphetamine. Representative analogs of the *N*-1,2(*R*)-diol series were evaluated for their

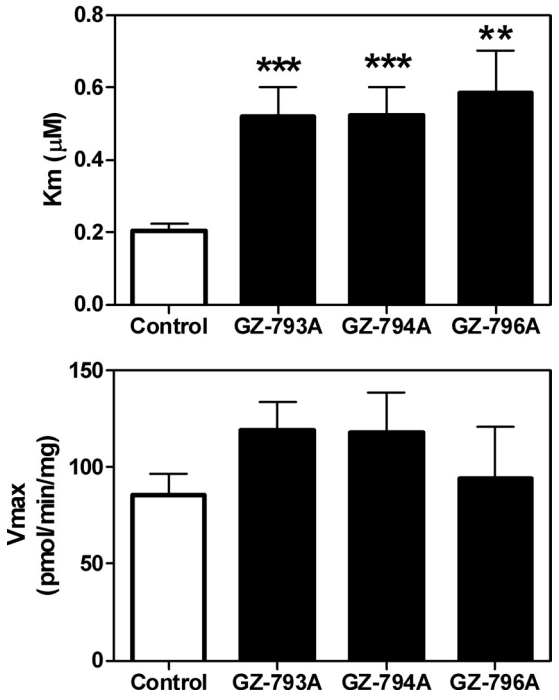

Fig. 7. *N*-1,2-Diol analogs competitively inhibit [^{3}H]DA uptake into vesicles prepared from rat striatum. Concentrations of GZ-793A (0.029 μM), GZ-794A (0.060 μM), and GZ-796A (0.79 μM) approximated the K_i values for inhibiting [^{3}H]DA uptake into isolated synaptic vesicles obtained from the data shown in Fig. 5. K_m (top) and V_{max} (bottom) values are mean ± S.E.M. **, $p < 0.01$ different from control; ***, $p < 0.001$ different from control (n = 4–7 rats/analog).

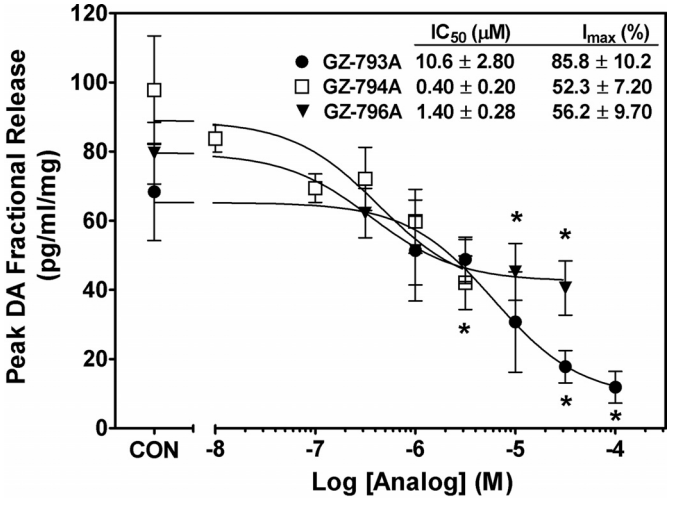

Fig. 8. In a concentration-dependent manner, GZ-793A, GZ-794A, and GZ-796A inhibit methamphetamine-evoked peak DA fractional release from striatal slices. Peak response data are expressed as mean ± S.E.M. pg/ml/mg of the slice weight. Slices were superfused with analog (10 nM-10 μM), and after a 10-min collection to determine intrinsic activity, methamphetamine (5 μM) was added to the buffer for 15 min. Analog remained in the buffer until the end of the experiment. *, $p < 0.05$ different from methamphetamine alone (control; CON) (n = 5 rats).

ability to decrease methamphetamine-evoked DA release in striatum. The leads, GZ-793A and GZ-794A, which exhibited the highest potency for inhibition of VMAT2 function, and GZ-796A, which inhibited VMAT2 function but not [^{3}H]DTBZ binding, were chosen for evaluation. All three *N*-1,2(*R*)-diol analogs did not evoke DA overflow in the absence of methamphetamine (had no intrinsic activity) and inhibited methamphetamine-evoked DA release in a concentration-dependent manner. These preclinical results support the further evaluation of these analogs for development as potential pharmacotherapies for methamphetamine abuse.

The current results suggest that GZ-793A, GZ-794A, and GZ-796A interact with VMAT2 to inhibit the pharmacological effects of methamphetamine. However, the order of potency for inhibition of VMAT2 function (GZ-793A = GZ-794A > GZ-796A) was different from the order of potency for inhibition of methamphetamine-evoked DA release (GZ-794A > GZ-796A > GZ-793A). Furthermore, correlation analysis with a limited number of structurally related compounds [GZ-793A, GZ-794A, GZ-796, lobelane, lobeline, mesotransdiene, *cis*-2,5-di-(2-phenethyl)-pyrrolidine hydrochloride (UKCP-110), and (3Z,5Z)-3,5-bis(2,4-dichlorobenzylidene)-1-methylpiperidine (UKMH-106)] for which data are available from both assays (current study; Miller et al., 2001, 2004; Beckmann et al., 2010; Nickell et al., 2010; Horton et al., 2011) reveal a lack of correlation between affinity for the inhibition of DA uptake at VMAT2 and the ability to inhibit methamphetamine-evoked DA release. There are several alternative explanations for this lack of correlation. First, variability in the physicochemical properties between the analogs may explain the lack of correlation between affinity for VMAT2 and efficacy for inhibition of methamphetamine-evoked DA release from slices. Such physicochemical properties are expected to differentially affect the ability of the analogs to distribute across cell membranes to reach its intracellular target. Furthermore, VMAT2 has greater accessibility in the vesicular preparation compared with the more intact slice preparation in which cell membranes impede analog accessibility.

Another possibility is that the analogs may be interacting with an alternate site on VMAT2 other than the DA uptake site to inhibit methamphetamine-evoked DA release. Research demonstrates that the extracellular and intracellular faces of DAT expresses distinct sites for DA translocation that are regulated differentially (Gnegy, 2003), which provides precedence for alternate recognition sites on VMAT2 that mediate uptake of DA and methamphetamine-evoked release of DA from the vesicle. Thus, the analogs may have different affinities for these alternative sites on VMAT2, which may explain the lack of correlation between affinity for VMAT2 and efficacy for inhibition of methamphetamine-evoked DA release from slices.

Further, the analogs may be interacting with an alternative target other than VMAT2, i.e., nicotinic receptors, to inhibit methamphetamine-evoked DA release. Lobeline interacts with both α4β2* and α7* nicotinic receptors (where * indicates putative nicotinic acetylcholine receptor subtype assignment); however, chemical defunctionalization (i.e., removal of the keto and hydroxyl groups from the phenyl ring side chains) of the lobeline molecule (affording analogs such as lobelane and the *N*-1,2-diol analogs) exhibit little or no affinity for α4β2* and α7* nicotinic receptors (Miller et al., 2001; Zheng et al., 2005; Beckmann et al., 2010; Horton et al., 2011). Furthermore, GZ-793A does not inhibit nicotinic receptors mediating nicotine-evoked DA release (unpublished observations). An alternative potential site of analog interaction is DAT. GZ-793A, GZ-794A, and GZ-796A exhibit affinity for DAT within the concentration range that inhibits methamphetamine-evoked DA release. However, the observation that GZ-793A is not self-administered in rats dimin-

TABLE 2
Summary of comparisons between phenyl ring substituted *N*-1,2-diol and respective *N*-methyl analog

Compound	Phenyl Ring Substituent	Configuration of the *N*-1,2-Diol	VMAT2 [^{3}H]DA Uptake (K_i)	Selectivity for VMAT over DAT or SERT	*N*-Methyl Analog	VMAT2 [^{3}H]DA Uptake (K_i)	Ratio of VMAT2 Uptake for the *N*-1,2-Diol Relative to the *N*-Methyl Analog	Ratio of VMAT2 Uptake for the *N*-1,2-Diol Relative to Lobelane
			μM			μM		
Lobelane	N.A.	N.A.	0.067	15.6	N.A.	N.A.	N.A.	N.A.
GZ-745A	No change	*R*	0.19	3.16	Lobelane	0.067	2.84	2.84
GZ-745B	No change	*S*	0.86	1.26			12.8	12.8
GZ-794A	Naphthalene	*R*	0.033	9.39	GZ-258C[a]	0.091[a]	0.36	0.49
GZ-794B	Naphthalene	*S*	0.080	2.00			0.88	1.19
GZ-796A	Biphenyl	*R*	0.79	6.70	GZ-272C[a]	0.034[a]	23.2	11.8
GZ-796B	Biphenyl	*S*	2.25	1.13			66.2	33.6
GZ-790A	3-Methoxy	*R*	0.14	22.4	GZ-261C[a]	0.030[a]	4.67	2.09
GZ-790B	3-Methoxy	*S*	0.52	12.8			17.3	7.76
GZ-792A	2-Methoxy	*R*	0.19	2.71	GZ-273C[a]	0.026[a]	7.31	2.84
GZ-792B	2-Methoxy	*S*	0.79	1.19			30.4	11.8
GZ-793A	4-Methoxy	*R*	0.029	49.7	GZ-252C[a]	0.015[a]	1.93	0.43
GZ-793B	4-Methoxy	*S*	0.18	18.9			12	2.69
GZ-797A	3,4-Methylene Dioxy	*R*	0.16	13.1	GZ-250C[a]	0.043[a]	3.72	2.39
GZ-797B	3,4-Methylene Dioxy	*S*	0.76	2.90			17.7	11.3
GZ-791A	3-Flouro	*R*	0.19	1.32	GZ-275C[a]	0.093[a]	2.04	2.84
GZ-791B	3-Flouro	*S*	1.03	0.60			11.1	15.4
GZ-795A	2,4-Dichloro	*R*	0.14	15.4	GZ-260C[a]	0.016[a]	8.75	2.09
GZ-795B	2,4-Dichloro	*S*	0.090	20.7			5.63	1.34

N.A., not applicable.
[a] Data taken from Nickell et al., 2011.

ishes support for an interaction with DAT as its mechanism of action (Beckmann et al., 2011). Finally, the observation that these analogs are 10- to 50-fold more potent at VMAT2 than at DAT provides support for VMAT2 as the pharmacological target.

Of the series, GZ-793A, the 4-methoxyphenyl *N*-1,2(*R*)-diol analog, exhibited the best profile with the greatest selectivity (50-fold) for VMAT2 and maximal inhibition (86%) of the effect of methamphetamine. The *N*-1,2(*R*)-diol moiety in GZ-793A improved water solubility compared with its *N*-methyl counterpart, GZ-252C. It is noteworthy that GZ-793A has been shown recently to decrease methamphetamine self-administration and methamphetamine conditioned-place preference, without altering food maintained responding (Beckmann et al., 2011), providing preclinical data that support its potential utility as a novel pharmacotherapy for methamphetamine abuse. Results from these preclinical studies provide support for GZ-793A as a lead compound in the search for pharmacotherapies to treat methamphetamine abuse.

Acknowledgments

We thank Agripina G. Deaciuc for excellent technical assistance.

Authorship Contributions

Participated in research design: Horton, Crooks, and Dwoskin.
Conducted experiments: Horton, Siripurapu, and Zheng.
Contributed new reagents or analytic tools: Zheng.
Performed data analysis: Horton, Siripurapu, and Zheng.
Wrote or contributed to the writing of the manuscript: Horton, Crooks, and Dwoskin.

References

Beckmann JS, Denehy ED, Zheng G, Crooks PA, Dwoskin LP, and Bardo MT (2011) The effect of a novel VMAT2 inhibitor, GZ-793A, on methamphetamine reward in rats. *Psychopharmacology*, doi:10.1007/s00213-011-2488-9.

Beckmann JS, Siripurapu KB, Nickell JR, Horton DB, Denehy ED, Vartak A, Crooks PA, Dwoskin LP, and Bardo MT (2010) The novel pyrrolidine nor-lobelane analog UKCP-110 [*cis*-2,5-di-(2-phenethyl)-pyrrolidine hydrochloride] inhibits VMAT2 function, methamphetamine-evoked dopamine release, and methamphetamine self-administration in rats. *J Pharmacol Exp Ther* **335:**841–851.

Cesura AM, Bertocci B, and Da Prada M (1990) Binding of [^{3}H]dihydrotetrabenazine and [^{125}I]azidoiodoketanserin photoaffinity labeling of the monoamine transporter of platelet 5-HT organelles. *Eur J Pharmacol* **186:**95–104.

Cheng Y and Prusoff WH (1973) Relationship between the inhibition constant (K1) and the concentration of inhibitor which causes 50 per cent inhibition (I50) of an enzymatic reaction. *Biochem Pharmacol* **22:**3099–3108.

Crooks PA, Zheng G, Vartak AP, Culver JP, Zheng F, Horton DB, and Dwoskin LP (2010) Design, synthesis and interaction at the vesicular monoamine transporter-2 of lobeline analogs: potential pharmacotherapies for the treatment of psychostimulant abuse. *Curr Top Med Chem* **11:**1103–1127.

Dar DE, Thiruvazhi M, Abraham P, Kitayama S, Kopajtic TA, Gamliel A, Slusher BS, Carroll FI, and Uhl GR (2005) Structure-activity relationship of trihexyphenidyl analogs with respect to the dopamine transporter in the on going search for a cocaine inhibitor. *Eur J Med Chem* **40:**1013–1021.

Di Chiara G and Imperato A (1988) Drugs abused by humans preferentially increase synaptic dopamine concentrations in the mesolimbic system of freely moving rats. *Proc Natl Acad Sci U S A* **85:**5274–5278.

Dwoskin LP and Crooks PA (2002) A novel mechanism of action and potential use for lobeline as a treatment for psychostimulant abuse. *Biochem Pharmacol* **63:**89–98.

Fischer JF and Cho AK (1979) Chemical release of dopamine from striatal homogenates: evidence for an exchange diffusion model. *J Pharmacol Exp Ther* **208:**203–209.

Gnegy ME (2003) The effect of phosphorylation on amphetamine-mediated outward transport. *Eur J Pharmacol* **479:**83–91.

Grabowski J, Roache JD, Schmitz JM, Rhoades H, Creson D, and Korszun A (1997) Replacement medication of cocaine dependence: methylphenidate. *J Clin Psychopharmacol* **17:**485–488.

Han DD and Gu HH (2006) Comparison of the monoamine transporters from human and mouse in their sensitivities to psychostimulant drugs. *BMC Pharmacol* **6:**6.

Harrod SB, Dwoskin LP, Crooks PA, Klebaur JE, and Bardo MT (2001) Lobeline attenuates D-methamphetamine self-administration in rats. *J Pharmacol Exp Ther* **298:**172–179.

Harrod SB, Dwoskin LP, Green TA, Gehrke BJ, and Bardo MT (2003) Lobeline does not serve as a reinforcer in rats. *Psychopharmacology (Berl)* **165:**397–404.

Horton DB, Siripurapu KB, Norrholm SD, Culver JP, Hojahmat M, Beckmann JS, Harrod SB, Deaciuc AG, Bardo MT, Crooks PA, et al. (2011) meso-Transdiene analogs inhibit vesicular monoamine transporter-2 function and methamphetamine-evoked dopamine release. *J Pharmacol Exp Ther* **336:**940–951.

Howell LL, Carroll FI, Votaw JR, Goodman MM, and Kimmel HL (2007) Effects of combined dopamine and serotonin transporter inhibitors on cocaine self-administration in rhesus monkeys. *J Pharmacol Exp Ther* **320:**757–765.

Institute of Laboratory Animal Resources (1996) *Guide for the Care and Use of Laboratory Animals* 7th ed. Institute of Laboratory Animal Resources, Commission on Life Sciences, National Research Council, Washington, DC.

Kilbourn M, Lee L, Vander Borght T, Jewett D, and Frey K (1995) Binding of α-dihydrotetrabenazine to the vesicular monoamine transporter is stereoselective. *Eur J Pharmacol* **278:**249–252.

Lehéricy S, Brandel JP, Hirsch EC, Anglade P, Villares J, Scherman D, Duyckaerts C, Javoy-Agid F, and Agid Y (1994) Monoamine vesicular uptake sites in patients with Parkinson's disease and Alzheimer's disease, as measured by tritiated dihydrotetrabenazine autoradiography. *Brain Res* **659:**1–9.

Liang NY and Rutledge CO (1982) Evidence for carrier-mediated efflux of dopamine from corpus striatum. *Biochem Pharmacol* **31:**2479–2484.

Liu Y and Edwards RH (1997) The role of vesicular transport proteins in synaptic transmission and neural degeneration. *Annu Rev Neurosci* **20:**125–156.

Miller DK, Crooks PA, Teng L, Witkin JM, Munzar P, Goldberg SR, Acri JB, and Dwoskin LP (2001) Lobeline inhibits the neurochemical and behavioral effects of amphetamine. *J Pharmacol Exp Ther* **296:**1023–1034.

Miller DK, Crooks PA, Zheng G, Grinevich VP, Norrholm SD, and Dwoskin LP (2004)

Lobeline analogs with enhanced affinity and selectivity for plasmalemma and vesicular monoamine transporters. *J Pharmacol Exp Ther* **310:**1035–1045.
Neugebauer NM, Harrod SB, Stairs DJ, Crooks PA, Dwoskin LP, and Bardo MT (2007) Lobelane decreases methamphetamine self-administration in rats. *Eur J Pharmacol* **571:**33–38.
Nickell JR, Krishnamurthy S, Norrholm S, Deaciuc G, Siripurapu KB, Zheng G, Crooks PA, and Dwoskin LP (2010) Lobelane inhibits methamphetamine-evoked dopamine release via inhibition of the vesicular monoamine transporter-2. *J Pharmacol Exp Ther* **332:**612–621.
Nickell JR, Zheng G, Deaciuc AG, Crooks PA, and Dwoskin LP (2011) Phenyl ring-substituted lobelane analogs: inhibition of [^{3}H]dopamine uptake at the vesicular monoamine transporter-2. *J Pharmacol Exp Ther* **336:**724–733.
Norrholm SD, Horton DB, and Dwoskin LP (2007) The promiscuity of the dopamine transporter: implications for the kinetic analysis of [^{3}H]serotonin uptake in rat hippocampal and striatal synaptosomes. *Neuropharmacology* **53:**982–989.
Owens MJ, Knight DL, and Nemeroff CB (2001) Second-generation SSRIs: human monoamine transporter binding profile of escitalopram and *R*-fluoxetine. *Biol Psychiatry* **50:**345–350.
Pifl C, Drobny H, Reither H, Hornykiewicz O, and Singer EA (1995) Mechanism of the dopamine-releasing actions of amphetamine and cocaine: plasmalemmal dopamine transporter versus vesicular monoamine transporter. *Mol Pharmacol* **47:**368–373.
Reith ME, Coffey LL, Xu C, and Chen NH (1994) GBR 12909 and 12935 block dopamine uptake into brain synaptic vesicles as well as nerve endings. *Eur J Pharmacol* **253:**175–178.
Substance Abuse and Mental Health Services Administration, Office of Applied Studies (2008) *Results from the 2007 National Survey on Drug Use and Health: National Findings*, NSDUH Series H-34, DHHS Publication SMA 08-4343, Substance Abuse and Mental Health Services Administration, Rockville, MD.
Sulzer D, Chen TK, Lau YY, Kristensen H, Rayport S, and Ewing A (1995) Amphetamine redistributes dopamine from synaptic vesicles to the cytosol and promotes reverse transport. *J Neurosci* **15:**4102–4108.
Sulzer D and Rayport S (1990) Amphetamine and other psychostimulants reduce pH gradients in midbrain dopaminergic neurons and chromaffin granules: a mechanism of action. *Neuron* **5:**797–808.
Sulzer D, Sonders MS, Poulsen NW, and Galli A (2005) Mechanisms of neurotransmitter release by amphetamines: a review. *Prog Neurobiol* **75:**406–433.
Tanda G, Newman AH, and Katz JL (2009) Discovery of drugs to treat cocaine dependence: behavioral and neurochemical effects of atypical dopamine transport inhibitors. *Adv Pharmacol* **57:**253–289.
Teng L, Crooks PA, and Dwoskin LP (1998) Lobeline displaces [^{3}H]dihydrotetrabenazine binding and releases [^{3}H]dopamine from rat striatal synaptic vesicles: comparison with D-amphetamine. *J Neurochem* **71:**258–265.
Teng L, Crooks PA, Sonsalla PK, and Dwoskin LP (1997) Lobeline and nicotine evoke [^{3}H]overflow from rat striatal slices preloaded with [^{3}H]dopamine: differential inhibition of synaptosomal and vesicular [^{3}H]dopamine uptake. *J Pharmacol Exp Ther* **280:**1432–1444.
Wise RA and Bozarth MA (1987) A psychomotor stimulant theory of addiction. *Psychol Rev* **94:**469–492.
Zheng G, Dwoskin LP, Deaciuc AG, Norrholm SD, and Crooks PA (2005a) Defunctionalized lobeline analogues: structure-activity of novel ligands for the vesicular monoamine transporter. *J Med Chem* **48:**5551–5560.
Zheng G, Dwoskin LP, Deaciuc AG, Zhu J, Jones MD, and Crooks PA (2005b) Lobelane analogues as novel ligands for the vesicular monoamine transporter-2. *Bioorg Med Chem* **13:**3899–3909.

Address correspondence to: Dr. Linda Dwoskin, College of Pharmacy, University of Kentucky, Lexington, KY 40536-0082. E-mail: ldwoskin@email.uky.edu